



OPEN *ZC3H12D* gene expression exhibits dual effects on the development and progression of lung adenocarcinoma

Yuansi Zheng¹, Yuhuan Zhang^{2,3}, Jieyi Li^{2,3}✉ & Ying Su¹✉

While precision oncology requires robust biomarkers, current predictors for lung adenocarcinoma (LUAD) often show limited clinical utility. This study investigates the multifaceted roles of *ZC3H12D*, a novel immunomodulatory molecule, in LUAD progression and tumor microenvironment regulation. Multi-omics analyses integrated *ZC3H12D* transcriptomic (511 tumors vs 59 normals), proteomic (74 tumors vs 69 normals), and single-cell RNA-seq data (15 tumors vs 11 normals). Immunohistochemistry validated *ZC3H12D* expression in 51 matched pairs. Computational biology approaches assessed immune infiltration, genomic instability (TMB/MSI/HRD), and pathway enrichment. Functional validation employed *ZC3H12D* knockdown in PC9 cells with colony formation and transwell assays. Multi-omics verification confirmed *ZC3H12D* upregulation in LUAD at both mRNA and protein levels ($p < 0.001$), with single-cell resolution revealing predominant localization in tumor-infiltrating immune cells. Moreover, *ZC3H12D* expression positively correlated with immune regulatory genes while inversely associating with genes involved in cellular respiration. Its expression was also linked to clinical markers such as TMB, MSI, HRD, tumor purity, and ploidy. Notably, high *ZC3H12D* expression revealed Immune-infiltrated microenvironment and favorable prognosis, despite silencing *ZC3H12D* resulted in significant inhibition of tumor cell proliferation and invasion in vitro ($p < 0.001$). Our findings demonstrate that high *ZC3H12D* expression in immune cells appears to enhance antitumor immune activity, whereas lower expression in malignant cells contributes to reduced cellular proliferation and migration. This spatial duality challenges conventional biomarker paradigms and provides mechanistic insights for developing cell type-targeted therapies.

Keywords Lung cancer, *ZC3H12D*, Cell proliferation, Cell migration, Dual effects

According to the latest statistics, lung cancer kills 350 people every day on average¹ and has created a significant public health problem in some developing countries. For example, the incidence of lung cancer is 3.7-fold higher in China than in the United States, while the mortality is 5.3-fold higher^{2,3}. Non-small cell lung cancer (NSCLC) constitutes approximately 85% of all lung cancers⁴; however, more than 80% of NSCLC patients are diagnosed with locally advanced or metastatic disease; due to the lack of effective therapeutic strategies, most of these patients are associated with a poor clinical outcome^{5,6}.

To predict the efficacy of treatment and achieve increased levels of patient stratification, multiple studies have attempted to identify specific molecular markers of NSCLC. For instance, patients with the *KRAS* p.G12 C mutation have been shown to achieve durable benefits from sotorasib therapy⁷. Furthermore, patients with high expression levels of *MYEOV* are known to be associated with a poor prognosis⁸. Other research identified a 19-gene signature (featuring *PEBP4*, *DKK1*, and *EDN3*) that is thought to be potentially valuable for the prognostic evaluation of patients with lung cancer⁹. However, most existing biomarkers have been identified from public databases by bioinformatic analysis and only a limited number of further verifications have been performed, thus limiting the clinical application of these biomarkers¹⁰.

¹Department of Pathology, Zhejiang Cancer Hospital, NO.1 East Banshan Road, Gongshu, Hangzhou 310022, China. ²Jiaying Key Laboratory of Precision Medicine and Companion Diagnostics, Jiaying Yunying Medical Inspection Co., Ltd, No.153 Huixin Road, Nanhu, Jiaying 314033, China. ³Department of R&D, Shanghai Yunying Biopharmaceutical Technology Co., Ltd, No.518 Xinzhuan Road, Songjiang, Shanghai 201612, China. ✉email: li@jieyi.life; suying@zjcc.org.cn

Among these markers, *ZC3H12* represents a particularly intriguing candidate. As a member of the CCCH-type zinc finger family¹¹, *ZC3H12* has been shown to negatively regulate Toll-like receptor (TLR) signaling and modulate macrophage activation¹², suggesting potential immunomodulatory functions shared across family members such as *ZC3H12D*¹³. Besides, *ZC3H12D* exhibits endonuclease activity through recognition of mRNA 3'UTR stem-loop structures, a process that can suppress cellular ubiquitination¹⁴. Given the established role of ubiquitination in promoting cell proliferation and survival¹⁵, these findings collectively suggest that *ZC3H12D* may exert complex regulatory effects in cancer biology. Clinically, *ZC3H12D* expression has demonstrated prognostic significance in multiple malignancies including head and neck squamous cell carcinoma^{16,17}, melanoma¹⁸, and lung adenocarcinoma¹⁹, although its precise tumor-specific mechanisms remain to be fully elucidated.

In this study, we aimed to elucidate the molecular mechanisms of *ZC3H12D* in lung cancer by investigating how different expression levels of *ZC3H12D* influence lung tumor cell behavior. Our findings advance the understanding of *ZC3H12D*'s prognostic value for lung cancer patients, and mechanistically establish that genetic perturbations engage a complex interactome of regulatory events, culminating in cell type-dependent functional antagonism. This complexity may account for the limited predictive value of some biomarkers in clinical settings.

Patients and methods

Public database analysis

RNAseq and phenotype data from 585 patients in the GDC TCGA Lung Adenocarcinoma database were downloaded using Xenabrowser ([https://xenabrowser.net/datapages/?cohort=GDC%20TCGA%20Lung%20Adenocarcinoma%20\(LUAD\)&removeHub=https%3A%2F%2Fxcena.treehouse.gi.ucsc.edu%3A443](https://xenabrowser.net/datapages/?cohort=GDC%20TCGA%20Lung%20Adenocarcinoma%20(LUAD)&removeHub=https%3A%2F%2Fxcena.treehouse.gi.ucsc.edu%3A443))²⁰. After processing the data with the R packages “tidyverse” and “dplyr”, 570 samples with detectable *ZC3H12D* gene expression were retained, including 511 tumor tissues and 59 normal tissues.

Proteomic data (PDC000153)²¹ were obtained from the CPTAC database (https://pdc.cancer.gov/pdc/browsers/filters/disease_type:Lung%20Adenocarcinoma). Following exclusion of samples with undetectable *ZC3H12D* expression, quantitative differential analysis was performed on the remaining 74 LUAD tissues and 69 matched normal controls.

For single-cell analysis, we obtained sequencing data from GSE131907 (<https://www.ncbi.nlm.nih.gov/geo/query/acc.cgi?acc=GSE131907>). A representative subset (3%) of the total 100,217 cells (57,222 cells from 15 tumor specimens; 42,995 cells from 11 normal specimens) was randomly subsampled (set.seed = 123) to ensure computational tractability. Data processing followed the original study's pipeline using R package “Seurat” for normalization, t-SNE visualization, and cell-type annotation, with the R package “inferCNV” confirming malignant status²². Ten independent replicates were performed to assess the robustness of randomization outcomes. *ZC3H12D* expression mapping identified 3,130 qualified cells (2,504 immune, 217 normal epithelial, 409 tumor).

The R package “corrplot” was used to calculate the correlation matrix between *ZC3H12D* expression and other genes. GO annotation and KEGG enrichment analyses were conducted using the “clusterProfiler” package²³, while the “survival” package was employed for survival model fitting and testing based on different levels of *ZC3H12D* expression. Additionally, the GEPIA (<http://gepia.cancer-pku.cn>)²⁴ online tool was used to generate a bodymap of *ZC3H12D* expression. Correlations between *ZC3H12D* and immune cell infiltration were analyzed using the “Immune Cell Analysis (TIMER)” module in Sangerbox (<http://sangerbox.com>)²⁵, while the “Immune Infiltration Analysis (Estimate)” module calculated StromalScore, ImmuneScore, ESTIMATEScore, and MicroenvironmentScore based on *ZC3H12D* expression for each sample. The “Gene Expression and Mutation Landscape” module was utilized to analyze the correlation between *ZC3H12D* and the genomic mutation landscape.

Patient inclusion and exclusion

Clinical tissue samples were sourced from the Zhejiang Cancer Hospital Biobank. A total of 51 samples were randomly selected from eligible cases collected between 2014 and 2020. Retrospective inclusion criteria comprised surgical tissue samples from patients with a confirmed histopathological diagnosis of LUAD, along with high-quality matched adjacent non-tumorous tissue samples. Patients with non-LUAD subtypes, biopsy tissue samples, or those without paired adjacent non-tumorous tissue samples were excluded.

Hematoxylin & eosin (HE) and immunohistochemistry (IHC) staining

In brief, paraffin-embedded tumor tissue specimens and paired para-cancerous specimens were divided into 4 μm sections and then stained with HE according to a standard protocol. In addition, we quantified the expression levels of *ZC3H12D* protein by IHC. IHC assays were performed using an automated analytical instrument (BenchMark ULTRA system, Roche, Basel, Switzerland); tissue sections were stained with 5-LO Polyclonal Antibody (YT0027, Immunoway, Texas, USA) in accordance with the manufacturer's protocol. Microscopic observation of tumor cells stained with HE and IHC staining was conducted and photographed using an optical microscope (BX43, Olympus, Tokyo, Japan). The proportion (%) of tumor cells and positive IHC staining were both evaluated and scored retrospectively by two experienced pathologists in an independent manner.

Cell cultures

We acquired the NSCLC cell line PC9 from the Center for Surgery and Public Health (CSPH). Cells were routinely grown and maintained in RPMI-1640 medium (Life Technologies, NY, USA), supplemented with 10% fetal bovine serum (FBS, Sigma, MO, USA) and 1% penicillin/streptomycin in a 37°C moist culture incubator with a 5% CO₂ atmosphere.

ZC3H12D siRNA synthesis and transformation

ZC3H12D siRNA was synthesized by Ribo Co. (Suzhou, China) and stored at -80°C . Prior to transformation, cells were seeded (1×10^8) and cultured in serum-free medium for 24 h. Cells were then treated with 50 nM of ZC3H12D siRNA (5'-GCAAGATGGAAATCTTCCA) or negative control sequence (diluted in RPMI-1640 medium) for 48 h. All protocols were carried out in strict accordance with the manufacturer's protocols.

Western blot analysis

Cells were harvested by centrifugation and lysed using radioimmunoprecipitation assay (RIPA) buffer (Beyotime, Shanghai, China) supplemented with 1 mM phenylmethylsulfonyl fluoride (PMSF). Equal amounts of protein (25 μg per sample) were separated by 10% SDS–polyacrylamide gel electrophoresis (SDS–PAGE) and subsequently subjected to immunoblotting. Primary antibodies were diluted 1:500 to 1:1000, with β -actin serving as a loading control. The ZC3H12D protein was detected using a ZC3H12D polyclonal antibody (Proteintech®, IL, USA; Cat. No. 24991–1-AP), and β -actin was detected using an anti- β -actin antibody [AC-15] (Abcam®, Cambridge, UK; Cat. No. ab6276). PageRuler™ Prestained Protein Ladder (Thermo Scientific™, MA, USA; Cat. No. 26616) was used as the molecular weight marker.

Clonogenic assay

In total, 500 to 1000 cells were seeded into 60 mm dishes and then treated with ZC3H12D siRNA or the negative control sequence. After treatment, cells were washed twice with complete medium for 48 h and then maintained in a 37°C incubator for 10–14 days. Colonies consisting of > 50 cells were considered as “surviving colonies” and scored directly using an inverted microscope after staining with crystal violet.

Invasion analysis

Transwell assays were used for invasion analysis. In brief, after treatment with ZC3H12D siRNA or the negative control sequence for 48 h, 5×10^4 cells were seeded into cell culture inserts with 1% FBS. Culture medium containing 10% FBS was placed outside the chambers. Cells that invaded the 10% FBS medium were visualized and counted after 48 h, as reported previously²⁶.

Statistical analysis

Differences between groups were assessed using one-way analysis of variance (ANOVA) in R (v4.2.2). Each experiment included three biological and technical replicates. Image analysis and quantification were conducted using ImageJ (NIH, NY, USA). Data are presented as mean \pm standard deviation. Statistical significance of group differences was determined using Student's t-test, while Poisson-based methods were employed to evaluate the relationships between variables. A p-value of < 0.05 was considered statistically significant. Figures were generated using the 'ggplot2' package in R, based on the statistical data²⁷.

Results

Patient characteristics

From 2014 to 2020, 51 patients with newly diagnosed NSCLC underwent surgical treatment at Zhejiang Cancer Hospital and were enrolled in this study. Among them, 26 were male (50.9%), with a mean age of 62 ± 9 years (range, 36–80 years; median, 63 years). Additionally, 22 patients (43.1%) were smokers, and 16 (31.4%) consumed alcohol regularly. Fourteen patients (27.5%) both smoked and drank, while the remaining 27 (52.9%) had no history of smoking or alcohol use. The distribution of patients across stages I, II, III, and IV was 31 (60.8%), 8 (15.7%), 2 (3.9%), and 4 (7.8%), respectively. Further participant characteristics are provided in Supplementary Table S1.

Expression profile of ZC3H12D in LUAD patients

The expression distribution of ZC3H12D across various tissues was analyzed using the GEPIA online tool. ZC3H12D was widely expressed in multiple major organs, with significantly elevated levels in hematologic malignancies and lymphomas compared to normal tissues (Fig. 1A), indicating its involvement in immune function beyond cell proliferation and growth regulation. Analysis of transcriptional levels in LUAD tumor and adjacent normal tissues from the TCGA database revealed a significant upregulation of ZC3H12D mRNA in tumors ($p < 0.00005$, Fig. 1B). This observation was further validated by quantifying ZC3H12D protein levels in tumor and paired normal tissues from 51 patients using IHC, showing a marked increase in protein expression in tumors ($p < 0.00005$, Fig. 1C, 1D). Consistent with these findings, proteomic analysis of LUAD specimens from the CPTAC database confirmed significantly elevated ZC3H12D protein levels in tumor tissues compared to matched normal controls ($p < 0.00005$, Fig. 1E). Consequently, the abnormal upregulation of ZC3H12D seems to be a molecular characteristic of LUAD. Notably, this upregulation was consistent across different ages (Fig. S1A) and genders (Fig. S1B) but was associated with tumor stage (Fig. S1C), with lower expression levels observed in late-stage tumors (stage III or IV) compared to early-stage tumors (stage I). This pattern underscores the complex role of ZC3H12D in LUAD progression.

Remarkably, the tumor tissue-wide upregulation of ZC3H12D masked important cellular heterogeneity. At single-cell resolution, immune cells demonstrated predominant ZC3H12D localization. Malignant cells exhibited non-significant elevation versus normal epithelium ($p > 0.05$, Fig. 1F). This spatial distribution suggests that ZC3H12D may exert its biological functions in LUAD primarily through modulation of the tumor immune microenvironment rather than via cell-autonomous mechanisms in cancer cells.

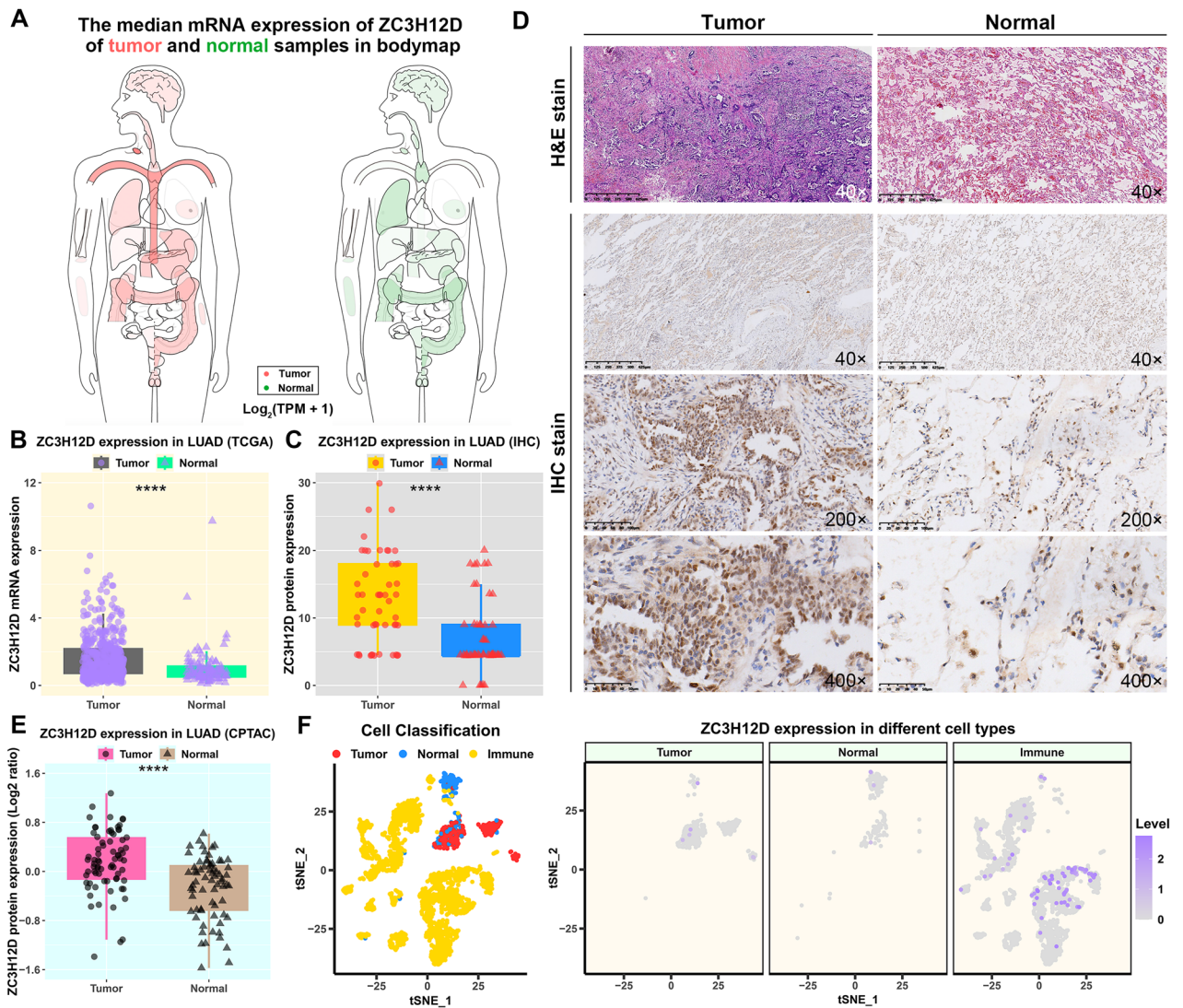


Fig. 1. *ZC3H12D* expression levels in lung tumor tissues and paired normal tissues. **A**), Bodymap illustrating *ZC3H12D* expression enrichment. Red denotes cancer patients, green denotes normal subjects, and the shading indicates expression levels; **B**), Differences in *ZC3H12D* expression between lung tumor and normal tissues. mRNA level differences were derived from LUAD RNAseq data in the TCGA database; **C**), protein level differences were assessed through quantitative immunohistochemistry (IHC) analysis of 51 matched lung adenocarcinoma tumor and adjacent normal tissues; **D**), Representative pathological staining and IHC results are presented; **E**), Proteomics differences of *ZC3H12D* between lung tumor and normal tissues, derived from CPTAC database; **F**), t-SNE plot of LUAD single cell transcriptomic data, illustrating distinct cellular clusters and the differential expression of *ZC3H12D* across various cell types. **** indicates $p < 0.00005$.

Co-expression gene set analysis of *ZC3H12D*

To explore the implications of *ZC3H12D* expression in LUAD, the top 100 genes most correlated with *ZC3H12D* levels in the TCGA transcriptomic data were analyzed (Table S2, Fig. 2A). GO functional annotation identified these genes as primarily involved in immune cell differentiation, activation, and proliferation, as well as membrane receptor family proteins (Fig. 2B). KEGG pathway enrichment analysis highlighted their significant involvement in immune cell signaling pathways and the NF- κ B pathway (Fig. 2C). Further analysis revealed that genes co-expressed with *ZC3H12D* are largely immune-related (Table S3, Fig. S2 A), while those negatively correlated with its expression are mainly associated with cellular respiration and mitochondrial function, particularly oxidative phosphorylation (Table S4, Fig. S2B). Collectively, these findings indicate that elevated *ZC3H12D* expression in LUAD is linked to enhanced cell proliferation and immune activation, with a concurrent impact on cellular energy metabolism.

Immune correlation analysis of *ZC3H12D*

The potential role of *ZC3H12D* in immune regulation was investigated by analyzing its expression correlation with known immune-regulatory genes and immune checkpoint genes. A total of 148 marker genes from five

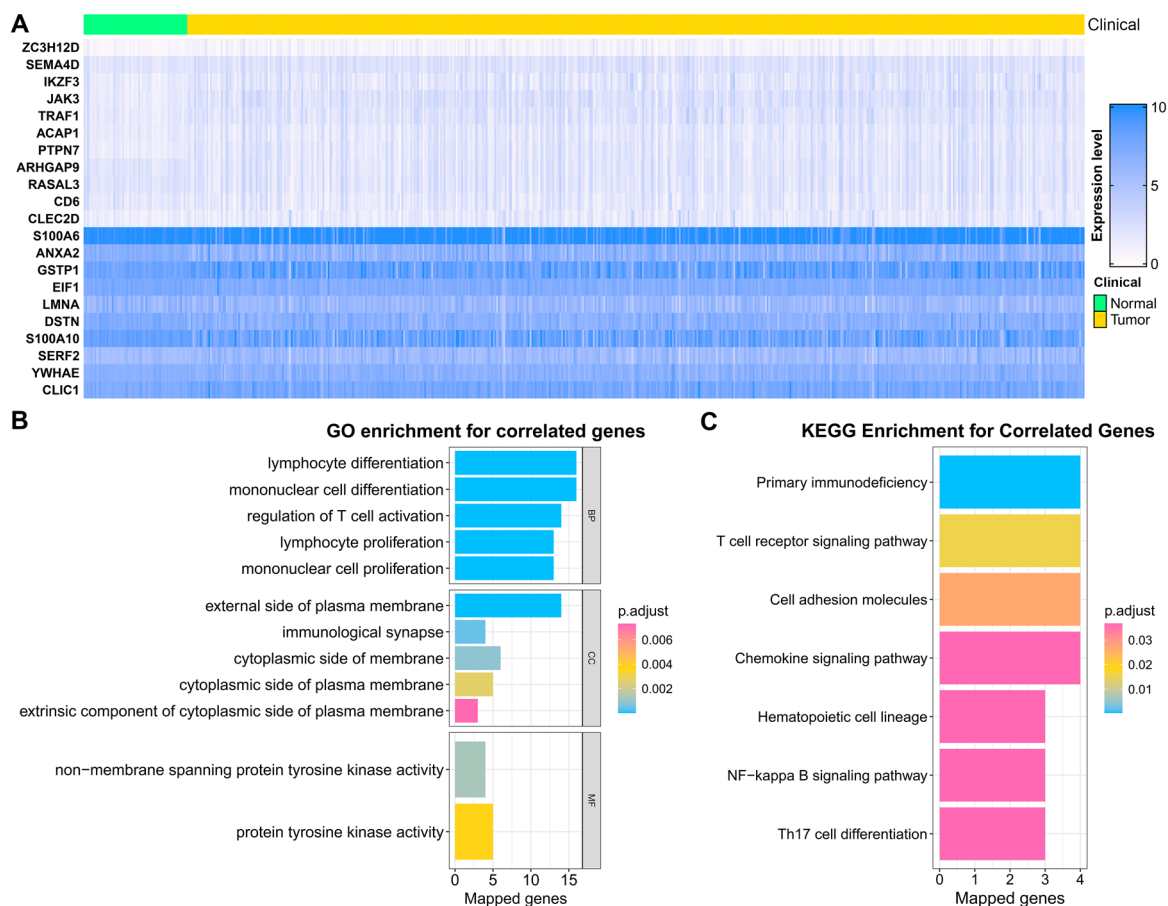


Fig. 2. Gene sets highly correlated with *ZC3H12D* expression and their functional analysis. **A**), Heatmap of the top 10 positively and negatively correlated genes with *ZC3H12D* expression; **B**), GO functional enrichment analysis of the top 100 genes most correlated with *ZC3H12D* expression; **C**), KEGG pathway enrichment analysis of the top 100 genes most correlated with *ZC3H12D* expression.

immune pathways were extracted from the expression matrix and correlated with *ZC3H12D* expression (Table S5). Genes with an absolute correlation coefficient greater than 0.3 and $p < 0.05$ were considered significantly correlated. Filtering by this threshold revealed that significantly correlated genes were more enriched in the receptor (61.11%, 11/18), immune stimulator (45.65%, 21/46), and immune inhibitor (37.5%, 9/24) pathways, compared to the chemokine (9.76%, 4/41) and MHC (9.52%, 2/21) pathways (Fig. 3A). Additionally, in the immune checkpoint pathways (Table S6), significantly correlated genes were more prevalent in the stimulatory (47.22%, 17/36) than the inhibitory (33.33%, 8/24) category (Fig. 3B). Notably, these genes exhibited positive correlations with *ZC3H12D*, suggesting a role in immune signaling within the tumor microenvironment, with a stronger stimulatory effect on the immune system.

This hypothesis was supported by an analysis using the Sangerbox online tool, which assessed the correlation between *ZC3H12D* expression and immune infiltration scores. The results indicated that *ZC3H12D* expression positively correlated with Stromal score, Immune score, and ESTIMATE score, as well as with immune microenvironment scores (Fig. 3C). The TIMER database corroborated these findings, showing associations between *ZC3H12D* expression and the infiltration of T cells, B cells, and dendritic cells (Fig. S3), highlighting the potential of high *ZC3H12D* expression to enhance immune microenvironment activation and immune cell infiltration.

Correlation of *ZC3H12D* expression with genomic mutation landscape in LUAD

Further analysis revealed an association between *ZC3H12D* and RNA modifications, particularly with the m6A and m5C types, within a set of 44 RNA modification marker genes comprising 10 m1A, 13 m5C, and 21 m6A genes (Table S7, Fig. S4). This association may influence the epigenetic modification landscape of the genome. To determine whether *ZC3H12D* expression correlates with the genomic mutation landscape in LUAD at the sequence level, patients were stratified into high and low expression groups based on median *ZC3H12D* expression levels, and mutation frequency differences across various genes were analyzed. Among 24 genes with significant differences in mutation frequency between the two groups and an overall mutation frequency exceeding 10%, missense mutations were the most common, followed by nonsense mutations and frameshift mutations (Fig. 4A).

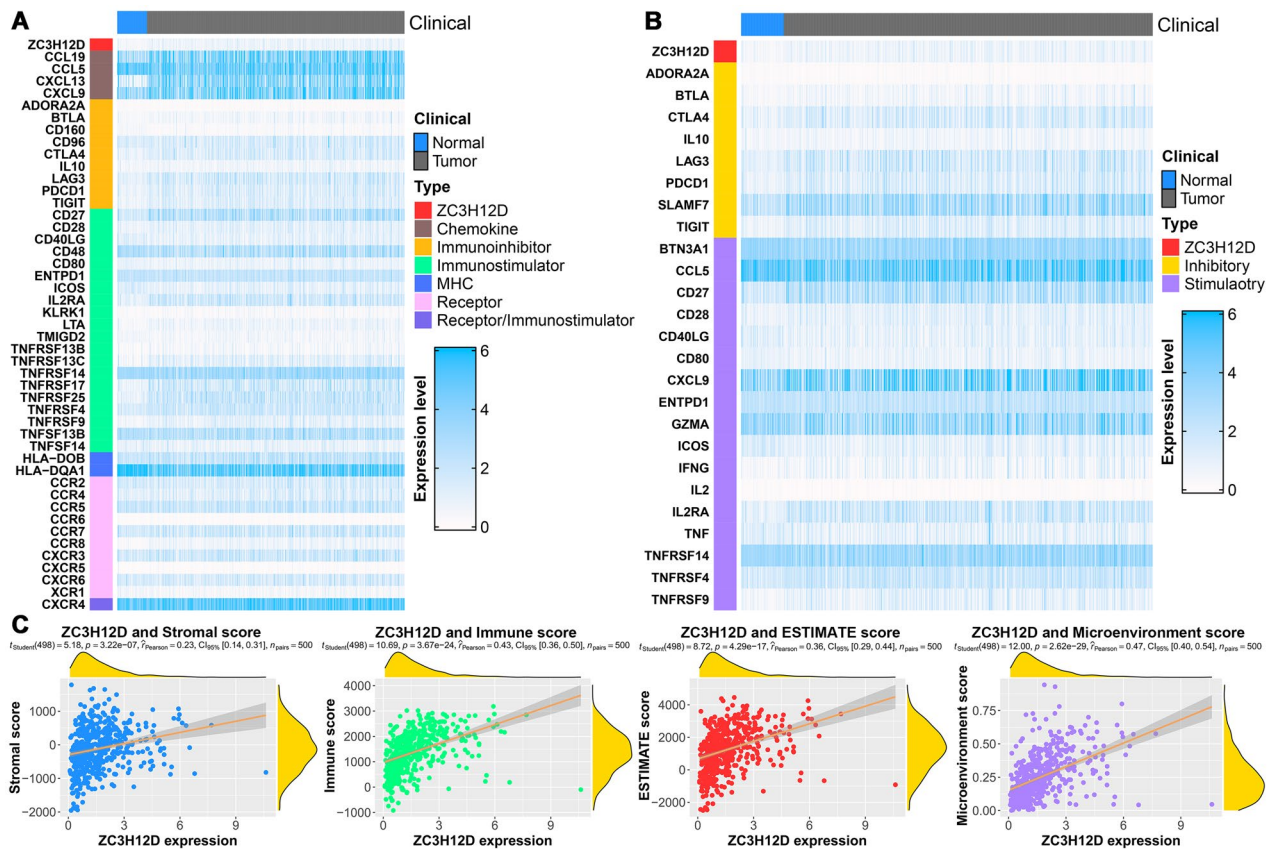


Fig. 3. Correlation analysis of *ZC3H12D* expression and immune function. **A**), Heatmap of immune regulatory genes significantly correlated with *ZC3H12D* expression; **B**), Heatmap of immune checkpoint genes significantly correlated with *ZC3H12D* expression; **C**), Correlation between *ZC3H12D* expression levels and immune infiltration scores in LUAD patients, including Stromal score, Immune score, ESTIMATE score, and Microenvironment score.

Interestingly, the mutation frequency of these 24 genes was significantly higher in the low *ZC3H12D* expression group compared to the high expression group. GO functional and KEGG pathway enrichment analyses revealed that these genes are involved in cell motility, microtubule assembly, cytoskeletal maintenance, and intracellular transport processes (Fig. 4B, 4C and 4D). These findings suggest that mutations and loss of function in these genes may impair cellular migration and disrupt intracellular transport due to abnormal motor protein and microtubule function, potentially leading to cell cycle arrest and reduced cell proliferation.

Association of *ZC3H12D* expression with genomic heterogeneity and patient survival

Although differential expression of *ZC3H12D* does not appear to drive high-frequency mutations in immune-related genes, a significant co-expression pattern with immune function gene clusters was observed. To further clarify the potential clinical relevance, the relationship between *ZC3H12D* expression and stratification indicators associated with immunotherapy strategies was evaluated. Significant differences were identified in tumor mutational burden (TMB), microsatellite instability (MSI), homologous recombination deficiency (HRD), as well as tumor purity and ploidy between groups with varying *ZC3H12D* expression levels (Fig. 5A). Additionally, distinct survival outcomes were noted among LUAD patients based on *ZC3H12D* expression levels, with higher expression correlating with better prognosis (Fig. 5B). These findings suggest that *ZC3H12D* expression may serve as a valuable prognostic indicator, particularly in the context of TMB, MSI, and other immunotherapy-related biomarkers.

Functional validation of *ZC3H12D* expression interference in vitro

Bioinformatic analysis indicates that low *ZC3H12D* expression is linked to mutations in genes involved in intracellular transport and cell motility, leading to impaired migration and proliferation, thereby inhibiting the tumorigenic process. Consequently, the elevated expression of *ZC3H12D* may serve as a characteristic feature of the molecular profile in tumor tissue. However, this increased expression is also associated with the activation of immune-related gene clusters, an enhanced immune microenvironment, and immune cell infiltration, while simultaneously suppressing genes related to cellular energy metabolism. These opposing effects suggest that *ZC3H12D* functions as a “double-edged sword” in tumor biology, where both high and low expression levels exert antagonistic influences on tumor cell survival.

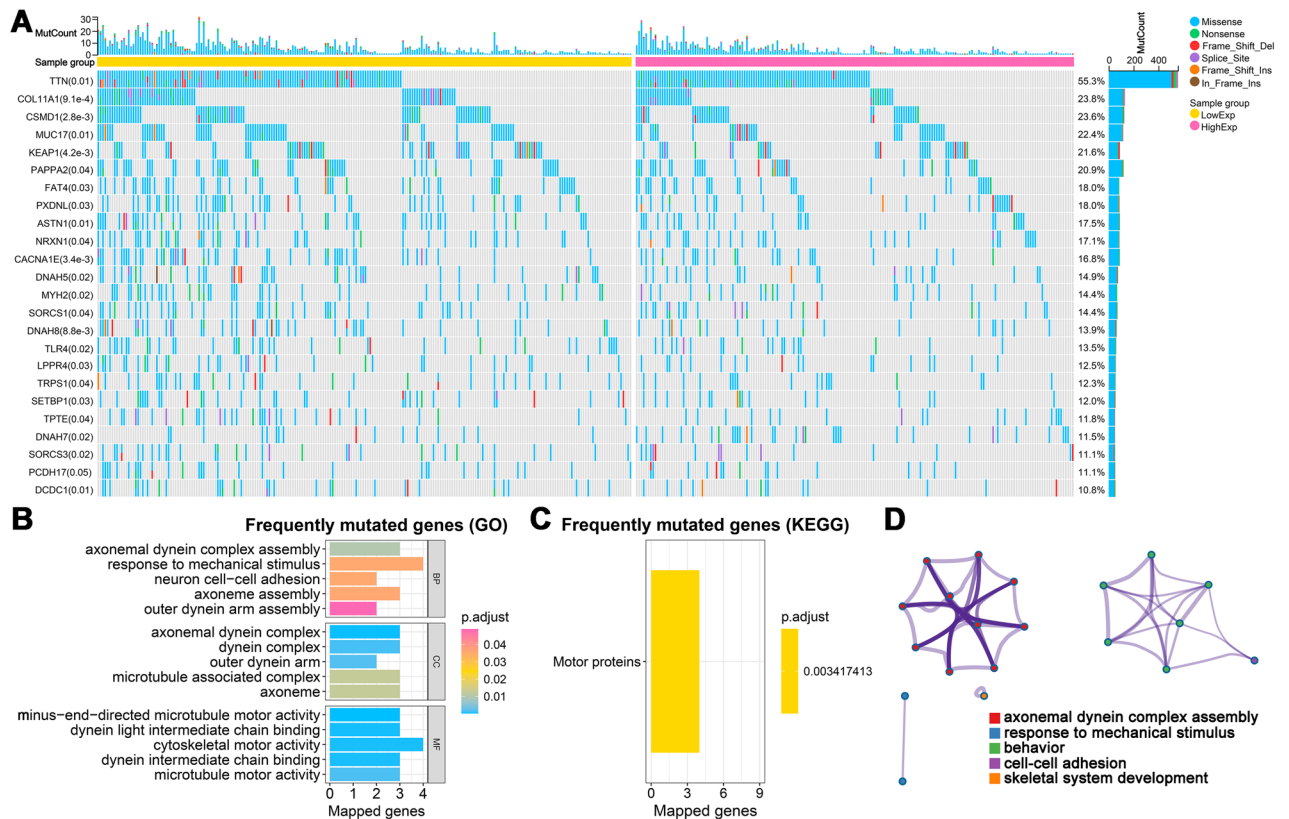


Fig. 4. Correlation analysis between *ZC3H12D* expression and the genomic mutation landscape. **A**), Mutation landscape of 24 genes with mutation frequencies greater than 10%, stratified by *ZC3H12D* expression levels. The numbers in parentheses next to gene names indicate the p-values for group differences; **B**), GO functional enrichment analysis of the 24 high-frequency mutated genes; **C**), KEGG pathway enrichment analysis of the 24 high-frequency mutated genes; **D**), Functional network diagram of the 24 high-frequency mutated genes. The size of each circular node is proportional to the number of genes, and the color indicates cluster identity. Similarity terms with a kappa score > 0.3 are linked by edges, with the thickness reflecting the score. Images were generated using the Metascape (<https://metascape.org>) online tool.

To validate the impact of low *ZC3H12D* expression on tumor cell behavior, synthetic siRNA targeting *ZC3H12D* was transfected into the LUAD cell line PC9 to achieve targeted gene knockdown. Western blot analysis confirmed a significant reduction in *ZC3H12D* expression in the siRNA-transfected group compared to the negative control ($p < 0.0005$, Fig. 6A and 6B). *ZC3H12D* knockdown resulted in impaired colony formation and a marked reduction in cell proliferation ($p < 0.00005$, Fig. 6C and 6D). As anticipated, Transwell migration assays revealed a significant inhibition of cell migration following *ZC3H12D* silencing ($p < 0.00005$, Fig. 6E and 6F). These results strongly support the notion that low *ZC3H12D* expression acts as a negative survival factor for tumor cells. However, the previously observed association between high *ZC3H12D* expression and improved patient survival, suggests that an active “hot” tumor immune microenvironment may be more crucial for therapeutic outcomes than merely suppressing the proliferation and migration of individual tumor cells.

Discussion

Our findings corroborate prior reports demonstrating predominant *ZC3H12D* expression enrichment in immune-related tissues, particularly spleen, blood, and lymph nodes¹². Through comprehensive analysis of public datasets, we observed consistent upregulation of *ZC3H12D* in LUAD tissues relative to normal lung controls at both transcriptional and translational levels. IHC validation using paired tumor-normal samples further confirmed this elevated expression pattern. Intriguingly, co-expression analysis revealed significant associations between *ZC3H12D* and multiple RNA modification regulators, suggesting its potential involvement in genomic methylation pathways. Given the established clinical utility of methylation markers for early lung cancer detection and differential diagnosis^{28,29}, these collective findings identify *ZC3H12D* upregulation as a characteristic genomic aberration in LUAD with potential diagnostic stratification value.

Besides, *ZC3H12D* is also widely known to participate in the regulation of immune and inflammatory responses^{30,31}. For example, Emming et al. reported that T lymphocytes are mechanistically regulated by a module consisting of miR-146a, *ZC3H12D* and the transcription factors (TFs) nuclear factor- κ B (NF- κ B) and BHLHE40, and that *ZC3H12D* acts as a negative regulator of cytokine expression and negatively regulated by BHLHE40³². As a result, the expression level of *ZC3H12D* may influence the immune infiltration of tumors¹³.

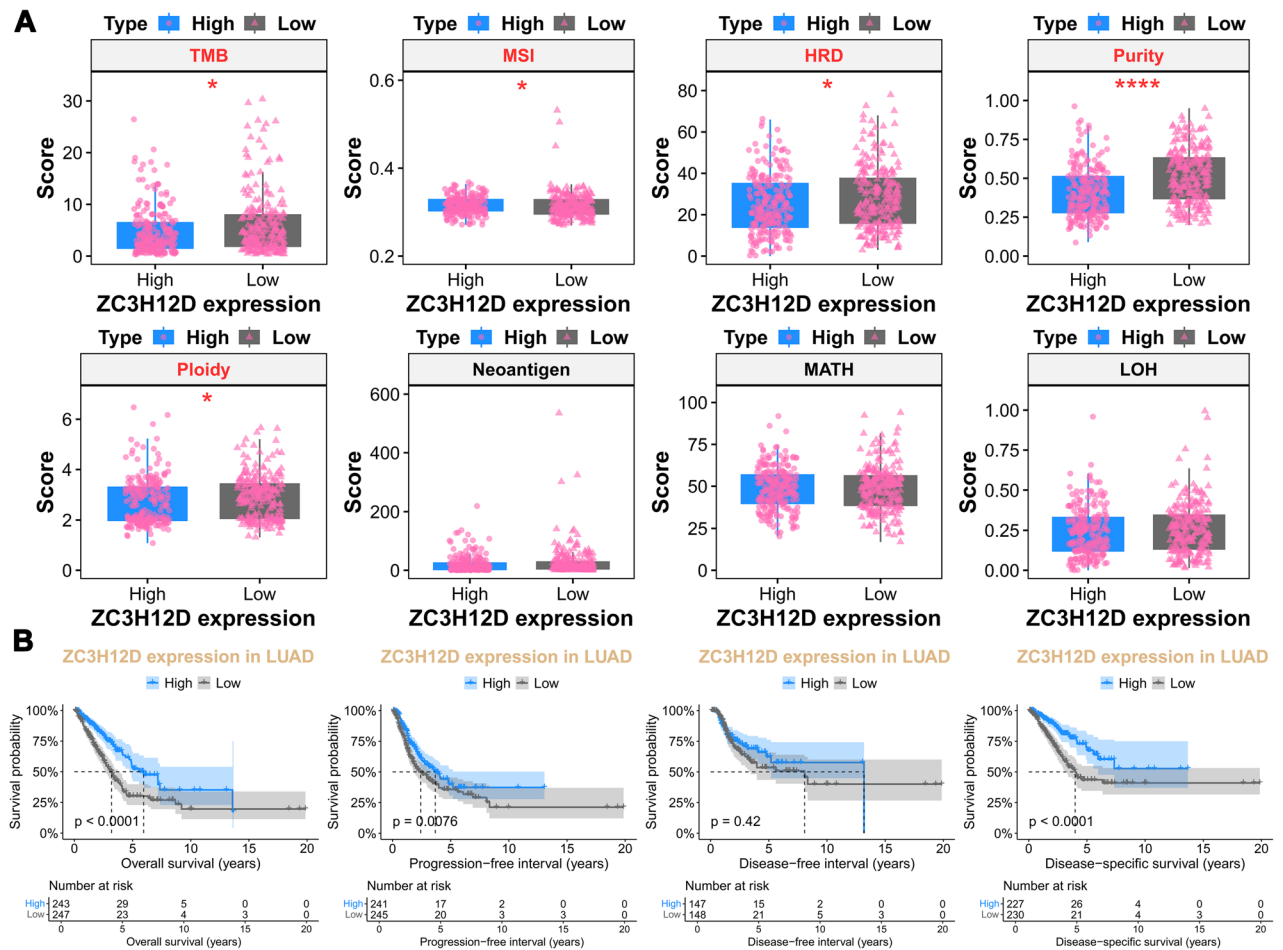


Fig. 5. Correlation analysis between *ZC3H12D* expression, genomic heterogeneity, and patient prognosis. **A**), Correlation between *ZC3H12D* expression levels and genomic heterogeneity metrics, including TMB (tumor mutation burden), MSI (microsatellite instability), HRD (homologous recombination deficiency), MATH (mutant-allele tumor heterogeneity), and LOH (loss of heterozygosity). * indicates $p < 0.05$; **** indicates $p < 0.00005$; **B**), Evaluation of the correlation between *ZC3H12D* expression levels and patient survival outcomes using four survival metrics: Overall survival (OS), Progression-free interval (PFI), Disease-free interval (DFI), and Disease-specific survival (DSS).

Our findings further support related research conclusions, as we discovered that genes positively correlated with *ZC3H12D* expression are primarily associated with immune signaling and immune cell activation. Additionally, *ZC3H12D* expression levels also show a positive correlation with immune cell infiltration. Therefore, building upon previous findings that *ZC3H12D* is involved in the regulation of both methylation and ubiquitination events, we speculate that *ZC3H12D* may affect the prognosis of patients by regulating mRNA, microRNA, long non-coding RNA (lncRNA), immune cells, and immune molecules³³.

Another line of evidence is our finding that *ZC3H12D* expression levels are significantly associated with MSI, TMB, HRD, and other genomic features. These characteristics are well-known predictive markers for the efficacy of clinical immunotherapies, such as immune checkpoint inhibitors, in LUAD patients. For instance, early-stage NSCLC patients with high TMB are more likely to achieve major or complete pathological response after treatment with PD-1/PD-L1 inhibitors^{34,35}. Although microsatellite instability-high (MSI-H) is rare in NSCLC, it remains an important reference for some clinicians when guiding immunotherapy decisions³⁶. Recently, HRD events have also been linked to better responses to neoadjuvant immunotherapy in lung cancer, suggesting that the status of homologous recombination pathway genes could serve as an additional marker for guiding neoadjuvant and immunotherapy decisions in NSCLC patients³⁷. Furthermore, LUAD patients with high aneuploidy and 9p chromosome loss possess a unique tumor immune microenvironment, which may make them less likely to benefit from immune checkpoint inhibitor therapies³⁸. Collectively, these findings underscore the potential correlation between *ZC3H12D* expression levels and clinical immunotherapy benefits, highlighting *ZC3H12D* as a promising target for the development of novel immune-based therapies across various cancers.

Interestingly, suppression of *ZC3H12D* expression appears to support the survival and proliferation of certain solid tumor cells. For example, *ZC3H12D* suppression has been shown to promote the progression of hepatocellular carcinoma³⁹ and enhance the proliferation of osteosarcoma cells⁴⁰. However, to our knowledge,

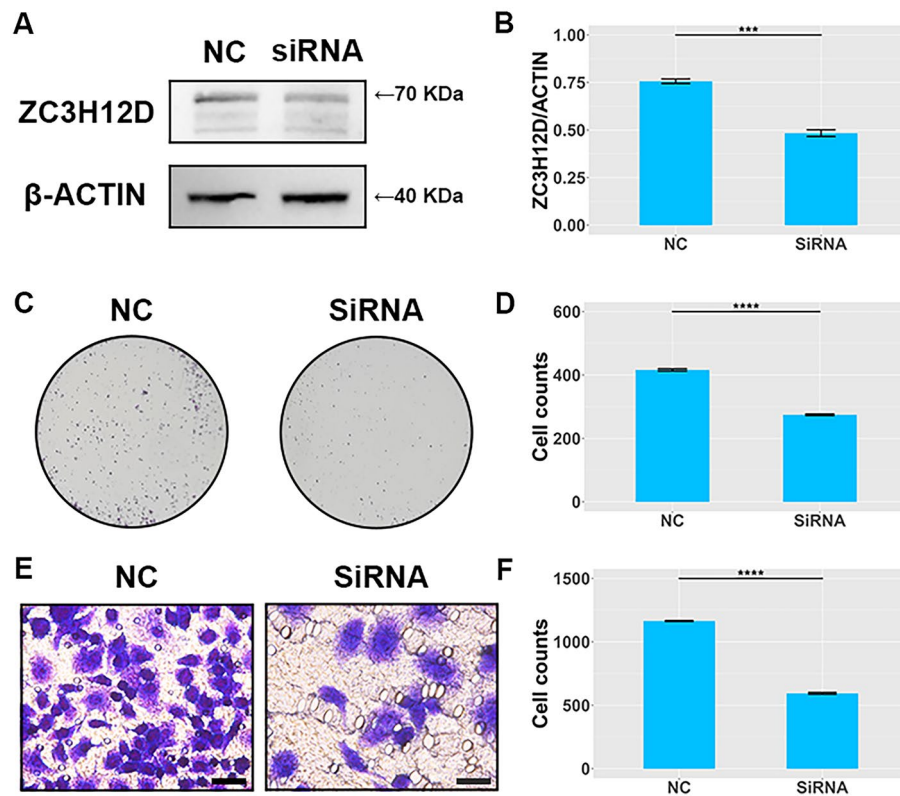


Fig. 6. Reduced *ZC3H12D* expression inhibits lung tumor cell proliferation and invasion. **A**), Western blot comparison between the siRNA group and the negative control (NC) group. *ZC3H12D* and β -ACTIN were detected on separate gels. The siRNA knockdown group was performed in triplicate with similar results across the three repeats. The band closest to the NC group was cropped and shown as a representative result. Full-length gels for both *ZC3H12D* and β -ACTIN are provided in Fig. S5; **B**), Bar plot displaying the quantitative analysis of western blot data; **C**), Clonogenic assay results comparing the siRNA group with the NC group; **D**), Bar plot illustrating the quantification of cell colonies; **E**), Transwell assay results comparing the siRNA group with the NC group, scale bar indicates 100 μ m (200 \times); **F**), Bar plot showing the quantification of invasive cells. *** indicates $p < 0.0005$; **** indicates $p < 0.00005$.

this study is the first to demonstrate that in LUAD, *ZC3H12D* expression levels are not only negatively correlated with gene sets involved in cellular respiration and oxidative phosphorylation but are also associated with an increased mutation frequency in genes responsible for intracellular material transport. This disruption may compromise the normal structure and function of motor proteins and microtubules. Consequently, high *ZC3H12D* expression could inhibit the energy metabolism of lung cancer cells, thereby suppressing cell proliferation, while simultaneously activating the host immune microenvironment, potentially limiting long-term tumor cell survival^{41–43}. Conversely, low *ZC3H12D* expression, while facilitating the creation of an ‘immune-desert’ inhibitory microenvironment, may impair intracellular transport and cell motility, ultimately affecting cell proliferation and migration^{44–46}, illustrating a “double-edged sword” effect. Our in vitro studies further demonstrated that *ZC3H12D* knockdown significantly reduces the proliferation and migration of lung cancer cells, suggesting that *ZC3H12D* is more likely to function as an oncogene rather than a tumor suppressor in LUAD.

Notably, our data demonstrate that high *ZC3H12D* expression in lung cancer tissues is significantly associated with an immunologically active tumor microenvironment and favorable patient prognosis, whereas in vitro knockdown of *ZC3H12D* in lung adenocarcinoma cells markedly suppresses tumor cell proliferation and migration. This discrepancy may arise from the limited resolution of bulk transcriptomic data in capturing the spatial distribution of *ZC3H12D*. Single-cell transcriptomic analysis showed that although *ZC3H12D* expression in malignant cells is slightly higher than in normal cells, its abundance is substantially greater in immune cell clusters than in stromal or malignant populations. These findings align with previous reports showing predominant *ZC3H12D* expression in T lymphocyte subsets, dendritic cells, monocytes, and macrophages, but minimal detection in fibroblasts, mast cells, or endothelial cells³³. Importantly, high *ZC3H12D* expression in immune cells enhances their tumor-killing activity, thereby reducing the risk of pulmonary metastasis in lung cancer⁴⁷. This compartmentalized expression pattern provides compelling reconfirmation a dual role for *ZC3H12D* in lung adenocarcinoma: low expression in malignant cells restricts their proliferative and migratory capacity, while high expression in tumor-infiltrating immune cells promotes immune activation and antitumor responses, ultimately improving patient survival.

However, this study has several limitations that should be acknowledged. First, we focused solely on the effects of *ZC3H12D* knockdown in lung tumor cells and did not assess the impact of enhanced *ZC3H12D* expression. Second, we conducted our experiments exclusively using the PC9 cell line, which may introduce selection bias due to the inherent differences between the in vivo and in vitro tumor microenvironments^{48,49}. Consequently, future studies should explore the effects of *ZC3H12D* overexpression across multiple tumor cell lines and model organisms, using upregulated *ZC3H12D* levels as a positive control.

In conclusion, we demonstrated that *ZC3H12D* expression is significantly upregulated in LUAD tissues compared to normal tissues. This upregulation primarily occurs in immune cell populations and may activate the immune microenvironment while inhibiting cellular energy metabolism. Conversely, downregulation of *ZC3H12D* increases the mutation frequency of genes involved in intracellular transport and motility, which suppresses lung cancer cell proliferation and migration. *ZC3H12D* exhibits a ‘double-edged sword’ effect in LUAD, with both high and low expression levels having distinct impacts on tumor cell survival. Notably, higher *ZC3H12D* expression could potentially serve as an independent predictor of clinical outcomes in LUAD patients, possibly due to a more active immune microenvironment. Overall, our study provides novel insights into the role of *ZC3H12D* in lung tumor cell behavior, deepening our understanding of its molecular mechanisms and potentially guiding the development of new therapeutic targets for lung cancer.

Data availability

The datasets used and/or analysed during the current study are available from the corresponding author on reasonable request. Transcriptome sequence data that support the findings have been deposited in the GDC TCGA Lung Adenocarcinoma ([https://xenabrowser.net/datapages/?cohort=GDC%20TCGA%20Lung%20Adenocarcinoma%20\(LUAD\)&removeHub=https%3A%2F%2Fxcena.treehouse.gi.ucsc.edu%3A443](https://xenabrowser.net/datapages/?cohort=GDC%20TCGA%20Lung%20Adenocarcinoma%20(LUAD)&removeHub=https%3A%2F%2Fxcena.treehouse.gi.ucsc.edu%3A443)), proteomic data deposited in the CPTAC database (https://pdc.cancer.gov/pdc/browse/filters/disease_type:Lung%20Adenocarcinoma), and single-cell sequencing data obtained from the GSE131907 study (<https://www.ncbi.nlm.nih.gov/gse/o/query/acc.cgi?acc=GSE131907>).

Received: 13 December 2024; Accepted: 12 May 2025

Published online: 18 May 2025

References

- Siegel, R. L., Miller, K. D., Fuchs, H. E. & Jemal, A. Cancer statistics, 2022. *CA Cancer J. Clin.* **72**(1), 7–33. <https://doi.org/10.3322/caac.21708> (2022).
- Zheng, R. et al. Cancer incidence and mortality in China, 2016. *J. Natl. Cancer Center.* <https://doi.org/10.1016/j.jncc.2022.02.002> (2022).
- Xia, C. et al. Cancer statistics in China and United States, 2022: profiles, trends, and determinants. *Chin. Med. J. (Engl.)* **135**(5), 584–590. <https://doi.org/10.1097/cm9.0000000000002108> (2022).
- Thai, A. A., Solomon, B. J., Sequist, L. V., Gainor, J. F. & Heist, R. S. Lung cancer. *Lancet* **398**(10299), 535–554. [https://doi.org/10.1016/S0140-6736\(21\)00312-3](https://doi.org/10.1016/S0140-6736(21)00312-3) (2021).
- Majeed, U., Manochakian, R., Zhao, Y. & Lou, Y. Targeted therapy in advanced non-small cell lung cancer: current advances and future trends. *J. Hematol. Oncol.* **14**, 108. <https://doi.org/10.1186/s13045-021-01121-2> (2021).
- Duma, N., Santana-Davila, R. & Molina, J. R. Non-small cell lung cancer: Epidemiology, screening, diagnosis, and treatment. *Mayo Clin. Proc.* **94**(8), 1623–1640. <https://doi.org/10.1016/j.mayocp.2019.01.013> (2019).
- Skoulidis, F. et al. Sotorasib for lung cancers with KRAS p. G12C mutation. *N. Engl. J. Med.* **384**, 2371–2381. <https://doi.org/10.1056/NEJMoa2103695> (2021).
- Zhang, R. & Ma, A. High expression of MYEOV reflects poor prognosis in non-small cell lung cancer. *Gene* **770**, 145337. <https://doi.org/10.1016/j.gene.2020.145337> (2021).
- Zhao, J. et al. Identification of a novel gene expression signature associated with overall survival in patients with lung adenocarcinoma: A comprehensive analysis based on TCGA and GEO databases. *Lung Cancer* **149**, 90–96. <https://doi.org/10.1016/j.lungcan.2020.09.014> (2020).
- Schegoleva, A. A. et al. Prognosis of different types of non-small cell lung cancer progression: Current state and perspectives. *Cell. Physiol. Biochem.* **55**(S2), 29–48. <https://doi.org/10.33594/000000340> (2021).
- Liang, J. et al. A novel CCCH-zinc finger protein family regulates proinflammatory activation of macrophages. *J. Biol. Chem.* **283**(10), 6337–6346. <https://doi.org/10.1074/jbc.M707861200> (2008).
- Huang, S. et al. The putative tumor suppressor Zc3h12d modulates toll-like receptor signaling in macrophages. *Cell. Signal.* **24**(2), 569–576. <https://doi.org/10.1016/j.cellsig.2011.10.011> (2012).
- Gong, W., Dai, W., Wei, H., Chen, Y. & Zheng, Z. ZC3H12D is a prognostic biomarker associated with immune cell infiltration in lung adenocarcinoma. *Transl. Cancer Res.* **9**(10), 6128–6142. <https://doi.org/10.21037/tcr-20-1465> (2020).
- Fu, M. & Blakeshear, P. J. RNA-binding proteins in immune regulation: A focus on CCCH zinc finger proteins. *Nat. Rev. Immunol.* **17**(2), 130–143. <https://doi.org/10.1038/nri.2016.129> (2017).
- Dang, F., Nie, L. & Wei, W. Ubiquitin signaling in cell cycle control and tumorigenesis. *Cell Death Differ.* **28**(2), 427–438. <https://doi.org/10.1038/s41418-020-00648-0> (2021).
- Lu, Y. et al. A novel prognostic model for oral squamous cell carcinoma: The functions and prognostic values of RNA-binding proteins. *Front. Oncol.* **11**, 592614. <https://doi.org/10.3389/fonc.2021.592614> (2021).
- Wang, L., Yang, G., Liu, G. & Pan, Y. Identification of lncRNA signature of Tumor-Infiltrating T Lymphocytes with potential implications for prognosis and chemotherapy of head and neck squamous cell carcinoma. *Front. Pharmacol.* **12**, 795205. <https://doi.org/10.3389/fphar.2021.795205> (2021).
- Li, Y. et al. Identification of potential prognostic biomarkers associated with cancer metastasis in skin cutaneous melanoma. *Front. Genet.* **12**, 687979. <https://doi.org/10.3389/fgene.2021.687979> (2021).
- Yang, B. et al. Zc3h12d, a novel of hypomethylated and immune-related for prognostic marker of lung adenocarcinoma. *J. Inflamm. Res.* **14**, 2389–2401. <https://doi.org/10.2147/jir.S304278> (2021).
- Goldman, M. J. et al. Visualizing and interpreting cancer genomics data via the Xena platform. *Nat. Biotechnol.* **38**(6), 675–678. <https://doi.org/10.1038/s41587-020-0546-8> (2020).
- Gillette, M. A. et al. Proteogenomic characterization reveals therapeutic vulnerabilities in lung adenocarcinoma. *Cell* <https://doi.org/10.1016/j.cell.2020.06.013> (2020).
- Kim, N. et al. Single-cell RNA sequencing demonstrates the molecular and cellular reprogramming of metastatic lung adenocarcinoma. *Nat. Commun.* **11**(1), 2285. <https://doi.org/10.1038/s41467-020-16164-1> (2020).

23. Wu, T. et al. clusterProfiler 4.0: A universal enrichment tool for interpreting omics data. *Innovation (Camb)*. **2**, 100141. <https://doi.org/10.1016/j.xinn.2021.100141> (2021).
24. Tang, Z. et al. GEPIA: A web server for cancer and normal gene expression profiling and interactive analyses. *Nucleic Acids Res.* **45**(W1), W98–w102. <https://doi.org/10.1093/nar/gkx247> (2017).
25. Shen, W. et al. Sangerbox: A comprehensive, interaction-friendly clinical bioinformatics analysis platform. *iMeta*. <https://doi.org/10.1002/imt2.36> (2022).
26. Pijuan, J. et al. In vitro cell migration, invasion, and adhesion assays: From cell imaging to data analysis. *Front. Cell Dev. Biol.* **7**, 107. <https://doi.org/10.3389/fcell.2019.00107> (2019).
27. Wickham, H. *ggplot2: elegant graphics for data analysis* (Springer, 2016).
28. Gao, Q. et al. Unintrusive multi-cancer detection by circulating cell-free DNA methylation sequencing (THUNDER): Development and independent validation studies. *Annals Oncol.: Off. J. Euro. Soc. Med. Oncol.* **34**(5), 486–495. <https://doi.org/10.1016/j.annonc.2023.02.010> (2023).
29. Yu, Z. et al. Lung tumor discrimination by deep neural network model CanDo via DNA methylation in bronchial lavage. *iScience*. **27**, 110079. <https://doi.org/10.1016/j.isci.2024.110079> (2024).
30. Zhang, H. et al. ZC3H12D attenuated inflammation responses by reducing mRNA stability of proinflammatory genes. *Mol. Immunol.* **67**, 206–212. <https://doi.org/10.1016/j.molimm.2015.05.018> (2015).
31. Minagawa, K. et al. Posttranscriptional modulation of cytokine production in T cells for the regulation of excessive inflammation by TFL. *J. Immunol.* **192**(4), 1512–1524. <https://doi.org/10.4049/jimmunol.1301619> (2014).
32. Emming, S. et al. A molecular network regulating the proinflammatory phenotype of human memory T lymphocytes. *Nat. Immunol.* **21**(4), 388–399. <https://doi.org/10.1038/s41590-020-0622-8> (2020).
33. Chen, W. et al. Identification of a ZC3H12D-regulated competing endogenous RNA network for prognosis of lung adenocarcinoma at single-cell level. *BMC Cancer* **22**, 115. <https://doi.org/10.1186/s12885-021-08992-1> (2022).
34. Oncology CSoc, Therapy ECoTV-t, Oncology CSoc, Cancer ECoN-sCL. Expert Consensus on Tumor Mutational Burden for Immunotherapy in Lung Cancer. *Chinese J. Lung Cancer*. 2021;24(11):743-752. <https://doi.org/10.3779/j.issn.1009-3419.2021.101.40>
35. Deng, H. et al. PD-L1 expression and Tumor mutation burden as Pathological response biomarkers of Neoadjuvant immunotherapy for Early-stage Non-small cell lung cancer: A systematic review and meta-analysis. *Crit. Rev. Oncol. Hematol.* **170**, 103582. <https://doi.org/10.1016/j.critrevonc.2022.103582> (2022).
36. Bie, F. et al. Research progress of Anti-PD-1/PD-L1 immunotherapy related mechanisms and predictive biomarkers in NSCLC. *Front. Oncol.* **12**, 769124. <https://doi.org/10.3389/fonc.2022.769124> (2022).
37. Zhou, Z. et al. Homologous recombination deficiency (HRD) can predict the therapeutic outcomes of immuno-neoadjuvant therapy in NSCLC patients. *J. Hematol. Oncol.* **15**(1), 62. <https://doi.org/10.1186/s13045-022-01283-7> (2022).
38. Alessi, J. V. et al. Impact of aneuploidy and chromosome 9p loss on tumor immune microenvironment and immune checkpoint inhibitor efficacy in NSCLC. *J. Thorac. Oncol.* **18**(11), 1524–1537. <https://doi.org/10.1016/j.jtho.2023.05.019> (2023).
39. Ye, J., Fu, Y., Wang, Z. & Yu, J. Long non-coding RNA FOXP4-AS1 facilitates the biological functions of hepatocellular carcinoma cells via downregulating ZC3H12D by mediating H3K27me3 through recruitment of EZH2. *Cell Biol. Toxicol.* <https://doi.org/10.1007/s10565-021-09642-9> (2021).
40. Zhu, M. et al. miR-128-3p serves as an oncogenic microRNA in osteosarcoma cells by downregulating ZC3H12D. *Oncol. Lett.* **21**(2), 152. <https://doi.org/10.3892/ol.2020.12413> (2021).
41. Gajewski, T. F., Schreiber, H. & Fu, Y.-X. Innate and adaptive immune cells in the tumor microenvironment. *Nat. Immunol.* **14**(10), 1014–1022. <https://doi.org/10.1038/ni.2703> (2013).
42. Fu, T. et al. Spatial architecture of the immune microenvironment orchestrates tumor immunity and therapeutic response. *J. Hematol. Oncol.* **14**(1), 98. <https://doi.org/10.1186/s13045-021-01103-4> (2021).
43. Mellman, I., Chen, D. S., Powles, T. & Turley, S. J. The cancer-immunity cycle: Indication, genotype, and immunotype. *Immunity* **56**(10), 2188–2205. <https://doi.org/10.1016/j.immuni.2023.09.011> (2023).
44. Hall, A. The cytoskeleton and cancer. *Cancer Metastasis Rev.* **28**, 5–14. <https://doi.org/10.1007/s10555-008-9166-3> (2009).
45. Nahacka, Z., Novak, J., Zabalova, R. & Neuzil, J. Miro proteins and their role in mitochondrial transfer in cancer and beyond. *Front. Cell Dev. Biol.* **10**, 937753. <https://doi.org/10.3389/fcell.2022.937753> (2022).
46. Nasimi Shad, A. et al. Role of microRNAs in tumor progression by regulation of kinesin motor proteins. *Int. J. Biol. Macromol.* **270**, 132347. <https://doi.org/10.1016/j.ijbiomac.2024.132347> (2024).
47. Yin, C., Kato, M., Tomita, T., Han, Y. & Hiratsuka, S. Suppression of CEBP δ recovers exhaustion in anti-metastatic immune cells. *Sci. Rep.* **13**(1), 3903. <https://doi.org/10.1038/s41598-023-30476-4> (2023).
48. Manini, I. et al. Role of Microenvironment in Glioma Invasion: What We Learned from In Vitro Models. *Int. J. Mol. Sci.* <https://doi.org/10.3390/ijms19010147> (2018).
49. Gambaro, G., Gaebler, M., Keilholz, U., Regenbrecht, C. R. A. & Silvestri, A. From chemotherapy to combined targeted therapeutics: in vitro and in vivo models to decipher intra-tumor heterogeneity. *Front. Pharmacol.* <https://doi.org/10.3389/fphar.2018.00077> (2018).

Author contributions

Yuansi Zheng: Methodology, Validation, Formal analysis, Investigation, Resources, Data curation, Writing - Original Draft, Project administration, Funding acquisition; Yuhuan Zhang: Methodology, Validation, Formal analysis, Investigation, Data curation, Writing - review and editing; Jieyi Li: Conceptualization, Methodology, Software, Formal analysis, Investigation, Data Curation, Writing - original draft, Writing - review and editing, Visualization, Supervision; Ying Su: Data curation, Supervision, Project administration. All authors read and approved the final manuscript.

Funding

This work was supported by the Zhejiang Provincial Medical and Health Science and Technology Project [2022KY098], the Natural Science Foundation of Zhejiang Province [LQ20H260003] and the Key Technology Innovation Projects of Jiaying [2024BZ20002].

Declaration

Competing interests

Yuhuan Zhang and Jieyi Li is employed by the Jiaying Yunying Medical Inspection Co., Ltd. and the Shanghai Yunying Biopharmaceutical Technology Co., Ltd. The remaining authors declare that the research was conducted in the absence of any commercial or financial relationships that could be construed as potential

conflicts of interest. Other Authors have no Competing interest.

Ethics approval

This retrospective study was conducted according to the principles of the Declaration of Helsinki by the World Medical Association. The study design was approved specifically by the Internal Review Board of the Zhejiang Cancer Hospital (Reference: IRB-2020–302). All participants who provided tissue specimens provided signed and informed consent for this retrospective study.

Additional information

Supplementary Information The online version contains supplementary material available at <https://doi.org/10.1038/s41598-025-02163-z>.

Correspondence and requests for materials should be addressed to J.L. or Y.S.

Reprints and permissions information is available at www.nature.com/reprints.

Publisher's note Springer Nature remains neutral with regard to jurisdictional claims in published maps and institutional affiliations.

Open Access This article is licensed under a Creative Commons Attribution-NonCommercial-NoDerivatives 4.0 International License, which permits any non-commercial use, sharing, distribution and reproduction in any medium or format, as long as you give appropriate credit to the original author(s) and the source, provide a link to the Creative Commons licence, and indicate if you modified the licensed material. You do not have permission under this licence to share adapted material derived from this article or parts of it. The images or other third party material in this article are included in the article's Creative Commons licence, unless indicated otherwise in a credit line to the material. If material is not included in the article's Creative Commons licence and your intended use is not permitted by statutory regulation or exceeds the permitted use, you will need to obtain permission directly from the copyright holder. To view a copy of this licence, visit <http://creativecommons.org/licenses/by-nc-nd/4.0/>.

© The Author(s) 2025